



## OPEN ACCESS

## EDITED BY

Francesco Dondi,  
Università degli Studi di Brescia, Italy

## REVIEWED BY

Maria Ricci,  
Cardarelli Hospital, Italy  
Di Yang,  
Chinese Academy of Medical Sciences and  
Peking Union Medical College, China

## \*CORRESPONDENCE

Ying Liang

✉ liangying\_473@163.com

Jun Zhao

✉ petcenter@126.com

<sup>†</sup>These authors have contributed equally to this work

RECEIVED 10 July 2025

ACCEPTED 25 August 2025

PUBLISHED 10 September 2025

## CITATION

Wumener X, Ye X, Zhao J, Zhang Y, E T, Zhao J and Liang Y (2025) Case Report: NUTM1-rearranged lung sarcoma: a rare case imaged with dynamic and static <sup>18</sup>F-FDG PET/CT.  
*Front. Oncol.* 15:1663104.  
doi: 10.3389/fonc.2025.1663104

## COPYRIGHT

© 2025 Wumener, Ye, Zhao, Zhang, E, Zhao and Liang. This is an open-access article distributed under the terms of the [Creative Commons Attribution License \(CC BY\)](#). The use, distribution or reproduction in other forums is permitted, provided the original author(s) and the copyright owner(s) are credited and that the original publication in this journal is cited, in accordance with accepted academic practice. No use, distribution or reproduction is permitted which does not comply with these terms.

# Case Report: NUTM1-rearranged lung sarcoma: a rare case imaged with dynamic and static <sup>18</sup>F-FDG PET/CT

Xieraili Wumener<sup>1†</sup>, Xiaoxing Ye<sup>2†</sup>, Jiuhui Zhao<sup>1†</sup>, Yarong Zhang<sup>1</sup>, Tuyu E<sup>3</sup>, Jun Zhao<sup>4\*</sup> and Ying Liang<sup>1\*</sup>

<sup>1</sup>Department of Nuclear Medicine, National Cancer Center/National Clinical Research Center for Cancer/Cancer Hospital & Shenzhen Hospital, Chinese Academy of Medical Sciences and Peking Union Medical College/Shenzhen Clinical Research Center for Cancer, Shenzhen, China,

<sup>2</sup>Department of Pathology, National Cancer Center/National Clinical Research Center for Cancer/Cancer Hospital & Shenzhen Hospital, Chinese Academy of Medical Sciences and Peking Union Medical College/Shenzhen Clinical Research Center for Cancer, Shenzhen, China, <sup>3</sup>Department of Radiology, National Cancer Center/National Clinical Research Center for Cancer/Cancer Hospital & Shenzhen Hospital, Chinese Academy of Medical Sciences and Peking Union Medical College/Shenzhen Clinical Research Center for Cancer, Shenzhen, China, <sup>4</sup>Department of Nuclear Medicine, Shanghai East Hospital Tongji University, Shanghai, China

**Background:** Nuclear protein of testis midline carcinoma family member 1 (NUTM1)-rearranged lung sarcomas are rare malignant malignancies. <sup>18</sup>F-fluorodeoxyglucose (FDG) positron emission tomography/CT (PET/CT) is widely used for the differential diagnosis and staging of malignant tumours. This study aimed to identify the static and dynamic features of <sup>18</sup>F-FDG PET/CT in NUTM1-rearranged lung sarcomas. **Case Description:** A 46-year-old male patient underwent a chest CT scan for trauma, which revealed a tumor in the hilum of the left lung. The patient also underwent dynamic (chest) and static (whole body) PET/CT scans. The dynamic and static <sup>18</sup>F-FDG PET/CT scans showed a tumor in the hilum of the left lung, with a size of 8.6x6.7 cm, an SUV<sub>max</sub> of 17.6 and a K<sub>i</sub> of 0.0668 ml/g/min. Final pathology and genetic testing confirmed NUTM1-rearranged lung sarcoma.

**Conclusions:** This case shows dynamic and static <sup>18</sup>F-FDG PET/CT and pathological features of NUTM1-rearranged lung sarcomas.

## KEYWORDS

NUTM1-rearranged lung sarcoma, <sup>18</sup>F-FDG, PET/CT, dynamic, CT

## 1 Introduction

Nuclear protein of testis midline carcinoma family member 1 (NUTM1)-rearranged lung sarcomas are rare malignant malignancies (1). Currently, there are very few reports on NUTM1-rearranged lung sarcomas. The few reports that exist tend to be case studies focusing on pathological features (2, 3). The imaging features of NUTM1-rearranged lung sarcoma have been under-recognised.

$^{18}\text{F}$ -fluorodeoxyglucose (FDG) positron emission tomography/CT (PET/CT) has been widely used for diagnosing and staging tumours, as well as evaluating their efficacy and prognosis. In recent years, with the development of molecular imaging technology, the application of dynamic PET imaging in oncology has attracted much attention. Dynamic PET scans extract physiological parameters that reveal pathophysiological mechanisms of disease more effectively (4). Therefore, dynamic quantitative metabolic parameters (e.g., Ki) are potentially advantageous in tumor differential diagnosis, efficacy assessment, and prognostic evaluation (5–9).

In this study, we report the clinical, lung cancer-related serum tumor markers, CT scan and dynamic+static  $^{18}\text{F}$ -FDG PET/CT features of a patient diagnosed with NUTM1-rearranged sarcoma by pathological and genetic test results to deepen the understanding of the imaging features of this disease.

## 2 Case presentation

A 46-year-old male patient underwent a chest CT scan for trauma. Figure 1 shows the patient's chest CT scan. The results of

the chest CT scan showed a tumor in the hilum of the left lung, size of 10.8×7.6 cm. The tumor exhibited moderate inhomogeneous enhancement on the enhancement scan and encroached upon the mediastinum, mediastinal lymph nodes (LN), pulmonary arteries and veins, and the pericardium. Multiple LNs in the supraclavicular and mediastinal regions bilaterally, the largest LN was located in the 4L region of the mediastinum, with a size of 2.5×1.8 cm. There are several solid nodules in the upper lobe of the left lung. The largest is located in the subpleura, with a size of 1.0×0.9 cm. The chest CT scan results suggest lung cancer, accompanied by partial LNs metastases and nodules in the left upper lobe of the lung that are suggestive of metastasis. Lung cancer related serum tumor markers were negative, including carcinoembryonic antigen (CEA, 1.72 ng/ml, 0–5.0 ng/ml), pro-gastrin-releasing peptide (Pro GRP, 27.90 pg/ml, <69.2 pg/ml), recombinant cytokeratin fragment antigen 21-1 (CYFRA21-1, 1.87 ng/ml, <3.3 ng/ml), carbohydrate antigen 125 (CA125, 14.1 U/ml, <35.0 U/ml), neuron-specific enolase (NSE, 15.24 ng/ml, <16.3 ng/ml), and squamous cell carcinoma antigen (SCC, 1.28 ng/ml, <2.7 ng/ml).

The patient underwent a dynamic (chest, 65 min) + static (whole body, 10–20 min)  $^{18}\text{F}$ -FDG PET/CT scan for definitive diagnosis and pre-treatment staging. Before the  $^{18}\text{F}$ -FDG injection,

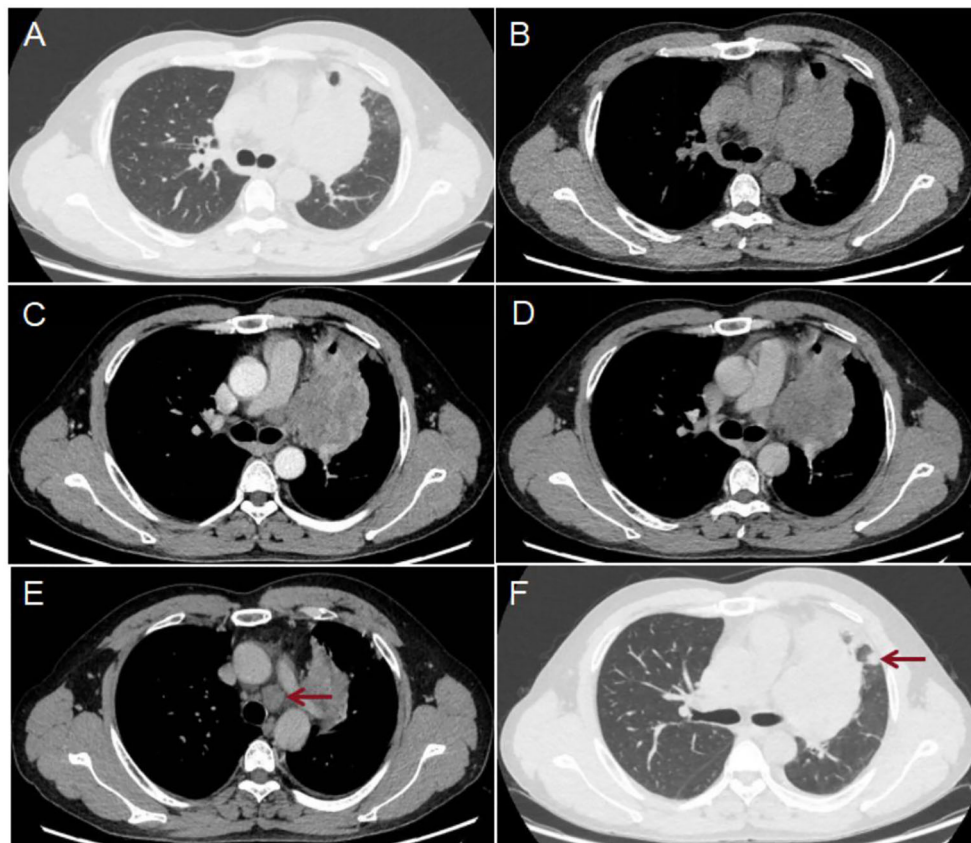


FIGURE 1

Results of the patient's chest CT scan: The scan showed a lesion in the hilum of the left lung (A, B), size of 10.8×7.6 cm. The enhanced scan [(C) arterial phase; (D) venous phase] shows moderate inhomogeneous enhancement. The largest LN was located in the 4L region of the mediastinum [(E) red arrow] and measured 2.5×1.8 cm. Several solid nodules were present in the upper lobe of the left lung, the largest of which was located subpleurally [(F) red arrow] and size of 1.0×0.9 cm.

the patient had fasted for at least 6 h and had a pre-scan glucose level of 6.1 mmol/L. PET scans of the chest region were initiated immediately after the injection of  $^{18}\text{F}$ -FDG (8.37 mCi) via an intravenous indwelling needle, according to the body mass index. The dynamic scans were carried out for a duration of 65 minutes. Dynamic scan data were then partitioned into 28 frames as follows:  $6 \times 10$  s,  $4 \times 30$  s,  $4 \times 60$  s,  $4 \times 120$  s, and  $10 \times 300$  s. Quantitative parameters ( $K_i$ ) was obtained through applying the irreversible two-tissue compartment model using in-house Matlab software. A whole-body static PET/CT scan was performed at the end of the dynamic acquisition process. Figures 2, 3 show the patient's dynamic and static  $^{18}\text{F}$ -FDG PET/CT scans of the patient. The dynamic and static  $^{18}\text{F}$ -FDG PET/CT scan showed a tumor in the hilum of the left lung (Figures 2A–D), with a size of  $8.6 \times 6.7$  cm (Figure 2D), an  $\text{SUV}_{\text{max}}$  of 17.6 (Figure 2B), and a  $K_i$  of 0.0668 ml/g/min (Figure 3A). Enlarged LNs in mediastinal regions 4R, 4L, and 5 with FDG-avid (Figures 2E, F), the largest LN was located in region 4L, with a size of  $2.6 \times 2.6$  cm, an  $\text{SUV}_{\text{max}}$  of 14.9 (Figure 2E), and a  $K_i$  of 0.0650 ml/g/min (Figure 3B). Furthermore, two nodules in the upper lobe of the left lung with FDG-avid (Figure 2G), the largest size of  $1.2 \times 1.1$  cm, with an  $\text{SUV}_{\text{max}}$  of 4.0 (Figure 2G), and a  $K_i$  of 0.0183 ml/g/min (Figure 3C).

The patient then underwent a bronchoscopic puncture biopsy. Final pathological and genetic test results confirmed NUTM1-rearranged lung sarcoma. Figure 4 shows the pathological morphology, immunohistochemical staining, and genetic testing results.

### 3 Discussion

NUTM1-rearranged lung sarcomas can occur at any age and are gender-neutral, with an atypical clinical presentation, aggressive nature and poor prognosis (2, 3). NUTM1-rearranged sarcomas have been reported with pathological features in a variety of different soft tissue sites in the body, including the stomach, kidneys, brain, ovaries and gastrointestinal tract (10–13). Most reports are dominated by case reports of the pathological features of NUTM1-rearranged lung sarcoma have been under-recognised.

In this case, we describe the clinical, CT, dynamic and static  $^{18}\text{F}$ -FDG PET/CT scan features of a patient diagnosed with NUTM1-rearranged lung sarcoma, as confirmed by pathological and genetic test results, to further our understanding of the imaging features of this disease. This is a 46-year-old male patient with an incidental finding of a lung tumour and no associated clinical manifestations. The chest CT scan showed a tumor in the hilum of the left lung and moderate inhomogeneous enhancement on the enhancement scan and invasion of adjacent tissues, reflecting the malignancy and invasiveness of the tumor. In addition, refinement lung cancer related serum tumor markers showed negative, including CEA, ProGRP, CYFRA21-1, CA125, NSE, and SCC.

The patient's static  $^{18}\text{F}$ -FDG PET/CT scan showed a tumor in the left lung and FDG-avid, an  $\text{SUV}_{\text{max}}$  of 17.6. The  $\text{SUV}_{\text{max}}$  value of the primary lesion was particularly suggestive of the malignancy of the disease. And the  $^{18}\text{F}$ -FDG PET/CT scan showed FDG-avid LNs in the mediastinal regions 4R, 4L, and 5 to help with accurate N

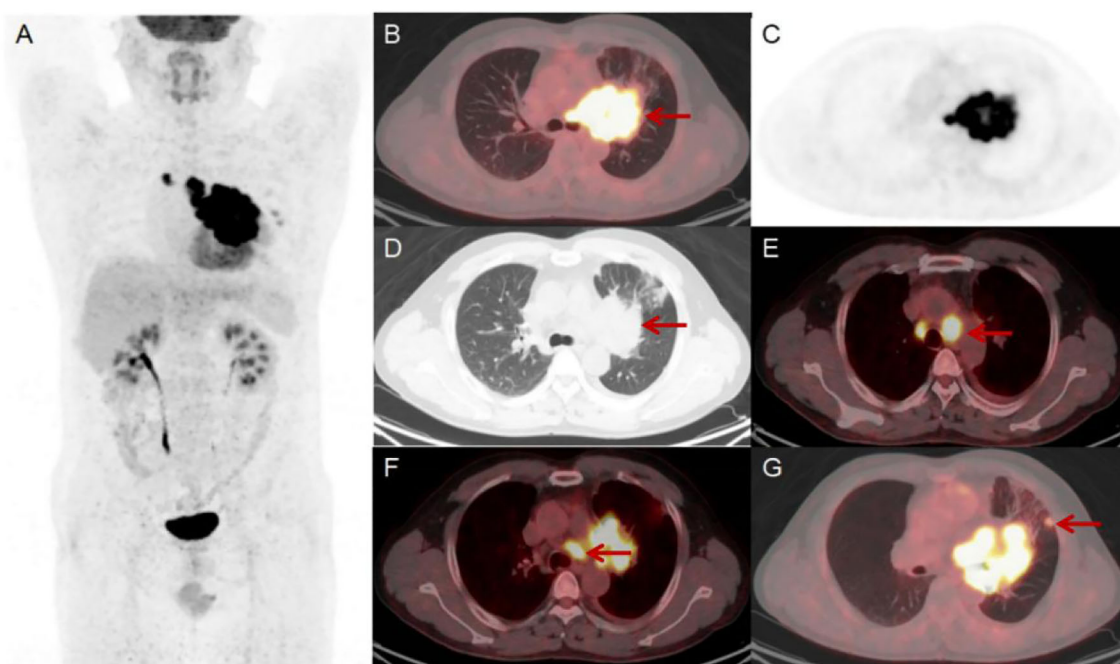


FIGURE 2

Results of the patient's static  $^{18}\text{F}$ -FDG PET/CT scan (A–G). The scan showed a lesion in the hilum of the left lung, size of  $8.6 \times 6.7$  cm [(D) red arrow] with an  $\text{SUV}_{\text{max}}$  of 17.6 [(B) red arrow]. There were enlarged LNs in mediastinal regions 4R, 4L and 5 that were FDG-avid [(E, F) red arrow]. The largest LN was located in region 4L and size of  $2.6 \times 2.6$  cm with an  $\text{SUV}_{\text{max}}$  of 14.9 [(E) red arrow]. Additionally, there were two FDG-avid nodules in the upper lobe of the left lung, the largest of which size of  $1.2 \times 1.1$  cm with an  $\text{SUV}_{\text{max}}$  of 4.0 [(G) red arrow].

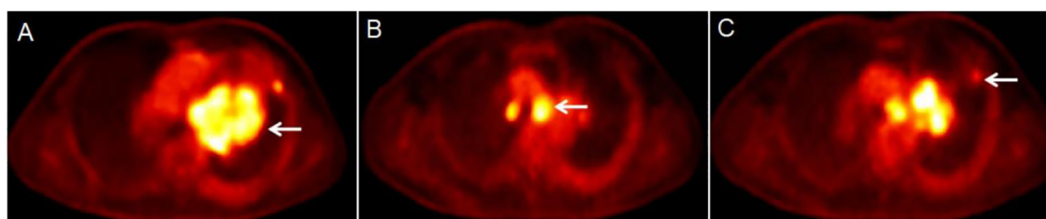


FIGURE 3

Results of the patient's dynamic  $^{18}\text{F}$ -FDG PET/CT scan (A-C). The dynamic  $^{18}\text{F}$ -FDG PET/CT scan showed a lesion in the hilum of the left lung [(A) white arrow], with a  $K_i$  of 0.0668 ml/g/min. The largest LN was located in region 4L [(B) white arrow], with a  $K_i$  of 0.0650 ml/g/min. The largest node was in the upper lobe of the left lung [(C) white arrow], with a  $K_i$  of 0.0183 ml/g/min.

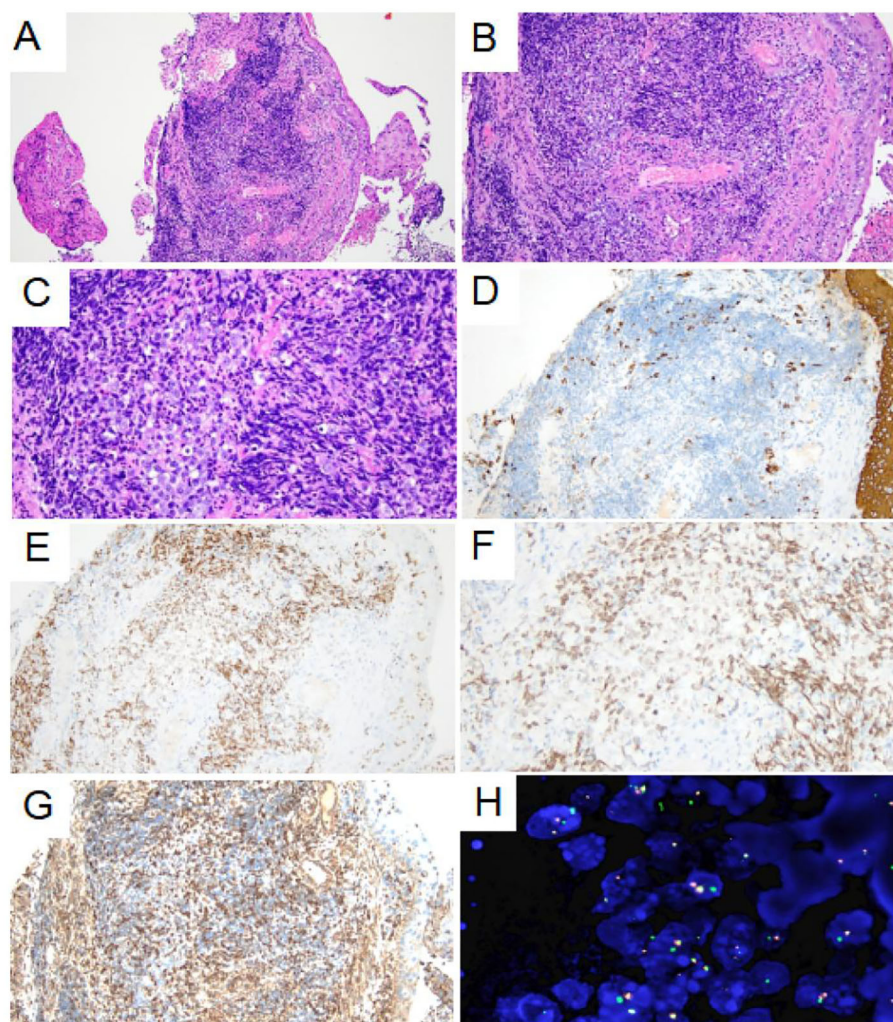


FIGURE 4

Pathological morphology and immunohistochemical staining of tumor. (A) Low-power histological examination (H&E stain, 100  $\times$ ) of bronchoscopy biopsy demonstrates that the tumor was located in the fibrous tissue of the bronchial mucosa. (B) At medium magnification, the tumor cells were distributed in sheet and nest shape, composed of monomorphic small round or short spindle cells, with little cytoplasm and most of the cytoplasm was transparent (H&E stain, 200  $\times$ ). (C) High-power of the tumor showed no obvious nuclear pleomorphism, fine chromatin, obvious nucleolus and mitoses are easily visible (H&E stain, 400  $\times$ ). (D) AE1/AE3 immunohistochemical staining showed negative expression of the tumor cell (200  $\times$ ). (E-F) NUT1 immunohistochemical staining showed moderately granular positive expression of tumor nucleus (200 $\times$  and 400 $\times$ ). (G) VIM immunohistochemical staining showed weak positive expression of tumor cell membrane and para-nuclear (200  $\times$ ). (H) Fluorescence *in situ* hybridization detection showed the presence of NUTM1 gene separation (1000  $\times$ ).

staging. Previous reports have shown that the disease tends to be highly aggressive and may be prone to distant metastasis (2, 3).  $^{18}\text{F}$ -FDG PET/CT also help with precise M-staging, which is important for managing the disease. As NUTM1-rearranged lung sarcoma is so rare, there are currently no relevant studies on imaging-based differential diagnosis. We believe that the  $^{18}\text{F}$ -FDG PET/CT features of NUTM1-rearranged lung sarcoma resemble those of NUT carcinoma (14) and SMARCA4-deficient NSCLC (15). However,  $^{18}\text{F}$ -FDG PET/CT is still mainly used to assist in TNM staging in these diseases and cannot yet be used for differential diagnosis based on imaging features. A pathological diagnosis is still required for the final diagnosis. In this case,  $^{18}\text{F}$ -FDG PET/CT scan ruled out distant metastases, helping clinicians to accurately stage patients and develop personalised treatment plans.

We previously conducted a series of studies on the value of dynamic  $^{18}\text{F}$ -FDG PET/CT in differential lung cancer diagnosis and N-staging (7–9). Our previous results have shown that, the dynamic metabolic parameter  $K_i$  has better differential diagnostic efficacy in the differential diagnosis of lung cancer, N-staging and prediction of EGFR status ( $K_i$  cut-off values, respectively: 0.0250 ml/g/min, 0.0220 ml/g/min, and 0.0350 ml/g/min), in particular, it improves specificity (7, 8). And, our study showed that, the average  $K_i$  in the lung malignant group (0.0267 ml/g/min) and metastatic lymph group (0.0190 ml/g/min) were higher than those in the lung benign group (0.0102 ml/g/min,  $P < 0.01$ ) and non-metastatic lymph group (0.0160 ml/g/min,  $P = 0.01$ ) (7, 8). In this case, we also further analysed the  $K_i$  values of the primary lung lesion, FDG-avid LNs, and subpleural nodes in the upper lobe of the left lung. Based on our previous research (7–9), we found that the  $K_i$  value of the primary lung foci (0.0668 ml/g/min) was significantly higher than the  $K_i$  value of the malignant lung group in our previous study ( $K_i$  cut-off value was 0.0250 ml/g/min), indicating the malignant nature of the disease. Among the mediastinal FDG-avid LNs, we measured the  $K_i$  value of a mediastinal region 4R (0.0650 ml/g/min), which was also significantly higher than the  $K_i$  value ( $K_i$  cut-off value was 0.0220 ml/g/min) of the metastatic LN in our previous study, also suggesting that this LN is a metastatic LN. In addition, we also measured the  $K_i$  of the nodules in the upper lobe of the left lung to be 0.0183 ml/g/min. Although we did not investigate the dynamic parameters of the metastatic lung lesions, the  $K_i$  trend also suggests malignancy of the nodule in the light of our previous experience in this area.

In terms of pathological features, tumors in the lungs characterized by small round cells with a sarcomatous morphology should be considered for undifferentiated small round cell sarcoma, lymphohematopoietic system tumors, and germ cell tumors. Therefore, panCK, CK8/18, VIM, CD20, CD3, CD99, CD34, CD117, MPO, SALL4 and BRG1 immunohistochemical staining tests were performed. The results showed that VIM exhibited punctate positive expression around the cell nucleus, and NUT exhibited positive expression in the cell nucleus. Therefore, a sarcoma with NUTM1 rearrangement was considered. Further FISH testing was conducted, which demonstrated separation of the NUTM1 gene. Thus, the pathological diagnosis was NUTM1 rearrangement sarcoma.

This case demonstrates the characteristics of NUTM1-rearranged lung sarcomas on  $^{18}\text{F}$ -FDG PET/CT and highlights the value of this imaging technique in the differential diagnosis and staging of malignant tumours. In the future, further attention will be paid to the mining of imaging features of NUTM1-rearranged lung sarcoma and the value of each metabolic parameter in differential diagnosis, staging, efficacy assessment and prognostic evaluation.

## 4 Conclusions

This case demonstrates the features of NUTM1-rearranged lung sarcomas on  $^{18}\text{F}$ -FDG PET/CT and highlights the value of this imaging technique in the differential diagnosis and staging of malignant tumours. The value of static and dynamic metabolic parameters in the differential diagnosis, staging, efficacy and prognostic assessment of NUTM1-rearranged lung sarcoma needs to be explored by collecting more cases.

## Data availability statement

The original contributions presented in the study are included in the article/supplementary material, further inquiries can be directed to the corresponding author/s.

## Ethics statement

The study was approved by the Ethics Committee of Cancer Hospital & Shenzhen Hospital, Chinese Academy of Medical Sciences and Peking Union Medical College. Written informed consent was obtained from the individual(s) for the publication of any potentially identifiable images or data included in this article.

## Author contributions

XW: Writing – original draft, Writing – review & editing. XY: Writing – original draft, Writing – review & editing. JHZ: Writing – review & editing. YZ: Data curation. TE: Writing – original draft. JZ: Writing – original draft, Writing – review & editing. YL: Writing – original draft, Writing – review & editing.

## Funding

The author(s) declare financial support was received for the research and/or publication of this article. This study was funded by National Cancer Center/National Clinical Research Center for Cancer/Cancer Hospital & Shenzhen Hospital, Chinese Academy of Medical Sciences and Peking Union Medical College, Shenzhen (E010322003, SZ2020MS008)/Shenzhen Clinical Research Center for Cancer and Shenzhen High-level Hospital Construction Found,

and the Shenzhen Municipal Basic Research Programme (Natural Science Foundation) Basic Research Project (20220525171717003).

## Conflict of interest

The authors declare that the research was conducted in the absence of any commercial or financial relationships that could be construed as a potential conflict of interest.

## Generative AI statement

The author(s) declare that no Generative AI was used in the creation of this manuscript.

## References

- McEvoy CR, Fox SB, Prall OWJ. Emerging entities in *NUTM1* -rearranged neoplasms. *Genes Chromosomes Cancer*. (2020) 59:375–85. doi: 10.1002/gcc.22838
- Zhu P, Sun K, Lao IW, Yu L, Bai Q, Zhou X, et al. Expanding the spectrum of *NUTM1*-rearranged sarcoma: A clinicopathologic and molecular genetic study of 8 cases. *Am J Surg Pathology*. (2024) 48:930–41. doi: 10.1097/PAS.0000000000002254
- Goto T, Arai Y, Shibata T, Oyama T, Yoshida A. Sarcoma with *MGA-NUTM1* fusion in the lung: an emerging entity. *Virchows Arch*. (2020) 476:317–22. doi: 10.1007/s00428-019-02623-8
- Rahmim A, Lodge MA, Karakatsanis NA, Panin VY, Zhou Y, McMillan A, et al. Dynamic whole-body PET imaging: principles, potentials and applications. *Eur J Nucl Med Mol Imaging*. (2019) 46:501–18. doi: 10.1007/s00259-018-4153-6
- Du F, Wumener X, Zhang Y, Zhang M, Zhao J, Zhou J, et al. Clinical feasibility study of early 30-minute dynamic FDG-PET scanning protocol for patients with lung lesions. *EJNMMI Phys*. (2024) 11:23. doi: 10.1186/s40658-024-00625-3
- Wumener X, Ye X, Zhang Y, Jin S, Liang Y. Dynamic and static 18F-FDG PET/CT imaging in *SMARCA4*-deficient non-small cell lung cancer and response to therapy: A case report. *Diagnostics*. (2023) 13:2048. doi: 10.3390/diagnostics13122048
- Wumener X, Zhang Y, Wang Z, Zhang M, Zang Z, Huang B, et al. Dynamic FDG-PET imaging for differentiating metastatic from non-metastatic lymph nodes of lung cancer. *Front Oncol [Internet]*. (2022) 12:1005924/full. doi: 10.3389/fonc.2022.1005924/full
- Wumener X, Zhang Y, Zang Z, Du F, Ye X, Zhang M, et al. The value of dynamic FDG PET/CT in the differential diagnosis of lung cancer and predicting EGFR mutations. *BMC Pulm Med [Internet]*. (2024) 24:227. doi: 10.1186/s12890-024-02997-9
- Wumener X, Zhang Y, Zang Z, Ye X, Zhao J, Zhao J, et al. The value of net influx constant based on FDG PET/CT dynamic imaging in the differential diagnosis of metastatic from non-metastatic lymph nodes in lung cancer. *Ann Nucl Med*. (2024) 38:904–12. doi: 10.1007/s12149-024-01964-y
- Diolaiti D, Dela Cruz FS, Gundem G, Bouvier N, Boulad M, Zhang Y, et al. A recurrent novel *MGA-NUTM1* fusion identifies a new subtype of high-grade spindle cell sarcoma. *Cold Spring Harb Mol Case Stud*. (2018) 4:a003194. doi: 10.1101/mcs.a003194
- Tamura R, Nakaoka H, Yoshihara K, Mori Y, Yachida N, Nishikawa N, et al. Novel *MXD4-NUTM1* fusion transcript identified in primary ovarian undifferentiated small round cell sarcoma. *Genes Chromosomes Cancer*. (2018) 57:557–63. doi: 10.1002/gcc.22668
- Dickson BC, Sung Y-S, Rosenblum MK, Reuter VE, Harb M, Wunder JS, et al. *NUTM1* gene fusions characterize a subset of undifferentiated soft tissue and visceral tumors. *Am J Surg Pathology*. (2018) 42:636–45. doi: 10.1097/PAS.0000000000001021
- Stevens TM, Morlote D, Xiu J, Swensen J, Brandwein-Weber M, Miettinen MM, et al. *NUTM1*-rearranged neoplasia: a multi-institution experience yields novel fusion partners and expands the histologic spectrum. *Modern Pathology*. (2019) 32:764–73. doi: 10.1038/s41379-019-0206-z
- Schlemmer AJ, Gorkiewicz G, Uggowitzer MM, Salamon S, Jost P, Talakic E. 18F-FDG PET/CT in *NUT* carcinoma of the thorax. *Clin Nucl Med [Internet]*. (2025). doi: 10.1097/RLU.0000000000005872
- Wumener X, Ye X, Zhang Y, E T, Zhao J, Liang Y, et al. *SMARCA4/BRG1*-deficient non-small cell lung cancer: clinical, imaging, pathological features, and follow-up results of 23 patients. *Transl Lung Cancer Res*. (2025) 14:107–23. doi: 10.21037/tlcr-24-567

Any alternative text (alt text) provided alongside figures in this article has been generated by Frontiers with the support of artificial intelligence and reasonable efforts have been made to ensure accuracy, including review by the authors wherever possible. If you identify any issues, please contact us.

## Publisher's note

All claims expressed in this article are solely those of the authors and do not necessarily represent those of their affiliated organizations, or those of the publisher, the editors and the reviewers. Any product that may be evaluated in this article, or claim that may be made by its manufacturer, is not guaranteed or endorsed by the publisher.